INTERFACE

royalsocietypublishing.org/journal/rsif

Report

Cite this article: Vittadello ST, McCue SW, Gunasingh G, Haass NK, Simpson MJ. 2019 Mathematical models incorporating a multi-stage cell cycle replicate normally-hidden inherent synchronization in cell proliferation. *J. R. Soc. Interface* **16**: 20190382.
http://dx.doi.org/10.1098/rsif.2019.0382

Received: 5 June 2019
Accepted: 26 July 2019

Subject Category:
Life Sciences–Mathematics interface

Subject Areas:
systems biology, biomathematics, computational biology

Keywords:
cell proliferation, synchronization, reproducibility, cell cycle, fluorescent ubiquitination-based cell cycle indicator, mathematical model

Author for correspondence:
Matthew J. Simpson
e-mail: matthew.simpson@qut.edu.au

†These authors contributed equally to the study.

Electronic supplementary material is available online at https://dx.doi.org/10.6084/m9.figshare.c.4608440.

THE ROYAL SOCIETY PUBLISHING

Mathematical models incorporating a multi-stage cell cycle replicate normally-hidden inherent synchronization in cell proliferation

Sean T. Vittadello[1], Scott W. McCue[1], Gency Gunasingh[2], Nikolas K. Haass[2,†] and Matthew J. Simpson[1,†]

[1]School of Mathematical Sciences, Queensland University of Technology, Brisbane, Queensland 4001, Australia
[2]The University of Queensland, The University of Queensland Diamantina Institute, Translational Research Institute, Woolloongabba, Brisbane, Queensland 4102, Australia

STV, 0000-0002-4476-6732; NKH, 0000-0002-3928-5360; MJS, 0000-0001-6254-313X

We present a suite of experimental data showing that cell proliferation assays, prepared using standard methods thought to produce asynchronous cell populations, persistently exhibit inherent synchronization. Our experiments use fluorescent cell cycle indicators to reveal the normally hidden cell synchronization, by highlighting oscillatory subpopulations within the total cell population. These oscillatory subpopulations would never be observed without these cell cycle indicators. On the other hand, our experimental data show that the total cell population appears to grow exponentially, as in an asynchronous population. We reconcile these seemingly inconsistent observations by employing a multi-stage mathematical model of cell proliferation that can replicate the oscillatory subpopulations. Our study has important implications for understanding and improving experimental reproducibility. In particular, inherent synchronization may affect the experimental reproducibility of studies aiming to investigate cell cycle-dependent mechanisms, including changes in migration and drug response.

1. Introduction

Cell proliferation is essential for a range of normal and pathological processes. Many different mathematical models of proliferation have been proposed [1–7]. It is often assumed that cells proliferate exponentially

$$\frac{\mathrm{d}M(t)}{\mathrm{d}t} = \lambda M(t), \quad M(t) = M(0)\,\mathrm{e}^{\lambda t}, \tag{1.1}$$

where $M(t)$ is the number of cells at time t and $\lambda > 0$ is the proliferation rate.

The eukaryotic cell cycle consists of four phases in sequence, namely gap 1 (G1), synthesis (S), gap 2 (G2) and mitosis (M) (figure 1*a*). A key assumption implicit in equation (1.1) is that the cell population is asynchronous, meaning that the cells are distributed randomly among the cell cycle phases (figure 1*b*), yielding a constant *per capita* growth rate, $(1/M(t))\,\mathrm{d}M(t)/\mathrm{d}t = \lambda$. By contrast, a population of cells is synchronous if the cells are in the same cell cycle phase (figure 1*c*), or partially synchronous if only a subpopulation of cells is synchronous (figure 1*d*). In this case, the synchronous cells divide as a cohort in discrete stages, producing a variable *per capita* growth rate. In addition to the implicit assumption of asynchronicity, classical exponential growth models and generalizations thereof [8] do not account for subpopulations, and predict monotonic population growth.

Here we provide new experimental data from two-dimensional cell proliferation assays in which the cell growth appears exponential as in equation (1.1). Unexpectedly, however, we observe oscillatory subpopulations arising from a phenomenon we refer to as *inherent* synchronization. We reveal the normally hidden inherent synchronization by identifying subpopulations based on cell

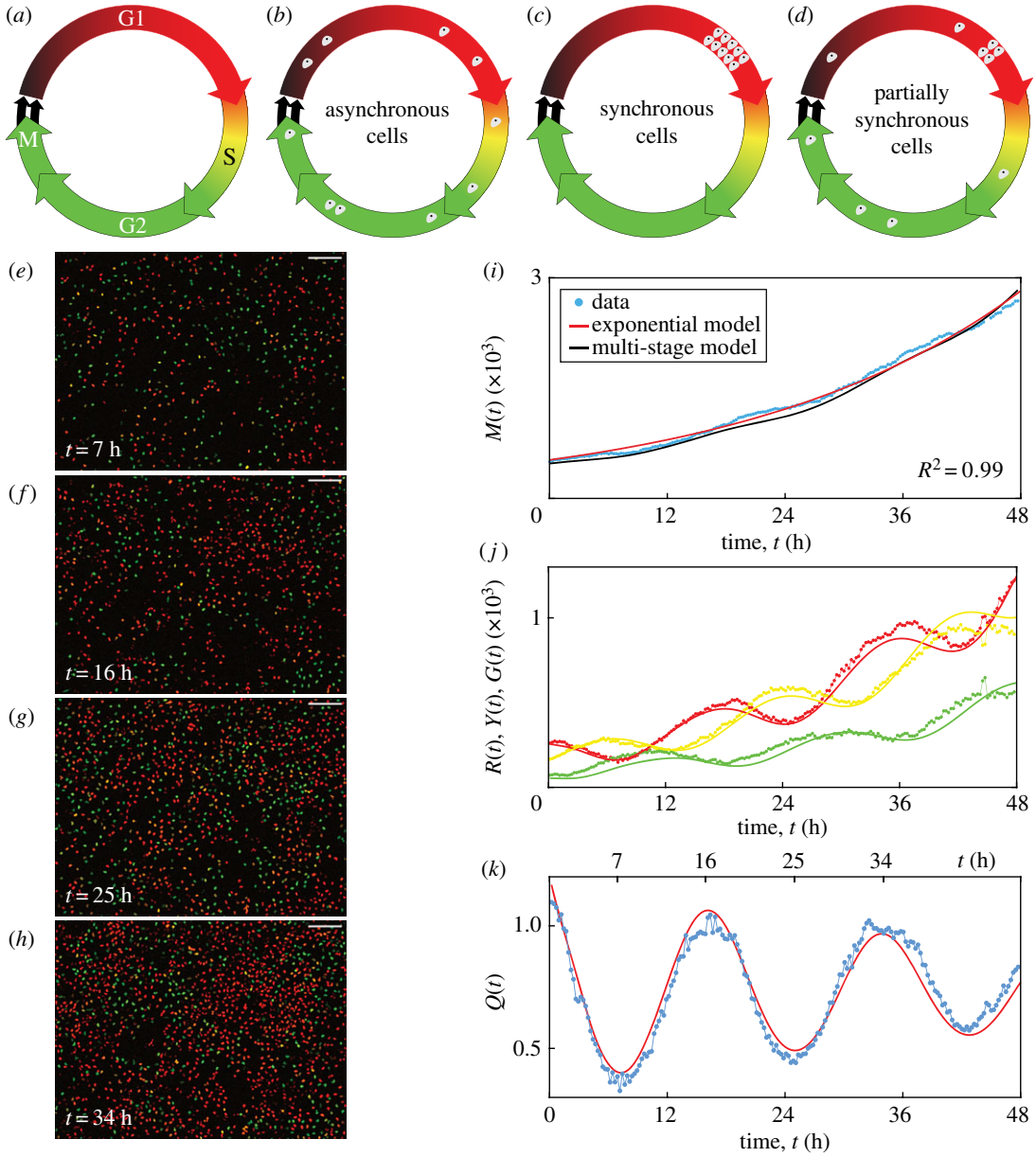

Figure 1. C8161 experimental data and multi-stage model solution. (*a*) The cell cycle, indicating the colour of FUCCI in each phase. (*b–d*) Asynchronous, synchronous and partially synchronous cells. (*e–h*) Images of a proliferation assay with FUCCI-C8161 cells. Scale bar, 200 µm. (*i*) $M(t)$. Linear regression of ln $M(t)$ versus t gives $R^2 = 0.99$. (*j*) $R(t)$, $Y(t)$ and $G(t)$. (*k*) $Q(t)$. Experimental data are shown as discs and the model solutions as curves. (Online version in colour.)

cycle phase, employing fluorescent ubiquitination-based cell cycle indicator (FUCCI) [9]. FUCCI enables visualization of the cell cycle of individual live cells via two sensors: when the cell is in G1 the nucleus fluoresces red, and when the cell is in S/G2/M the nucleus fluoresces green. During the G1/S transition, called early S (eS), both sensors fluoresce and the nucleus appears yellow (figure 1*a*). We explain these seemingly inconsistent observations by applying a multi-stage mathematical model for cell proliferation.

Previous studies of cell synchronization using FUCCI induce the synchronization using methods including serum starvation, cell cycle-inhibiting drugs, environmental pH or contact inhibition [10–15]. Our assays are prepared using a standard method [10] normally thought to produce asynchronous populations, and we take utmost care to ensure that there is no induced synchronization in our cell cultures due to serum starvation, low pH or contact inhibition (electronic supplementary material, S1). Over three cell lines and four independent experiments, however, we consistently observe inherent synchronization.

Neglecting synchronous subpopulations can have important implications for experiment reproducibility. For example, the accurate experimental evaluation of cell cycle-inhibiting drugs is highly dependent on the cell cycle distribution of the cell population [10,16]. In a partially synchronous population, the drug may have a delayed or advanced effect compared with an asynchronous population, depending on the cell cycle position of the synchronous cells. Generally, the presence of synchronization may affect the reproducibility of experiments that investigate cell cycle-dependent mechanisms, such as changes in migration and drug response. Revealing any synchronization with quantitative techniques like FUCCI will lead to a better understanding of these mechanisms.

2. Results

2.1. Experimental data

Our experimental data are time-series images from two-dimensional proliferation assays using three melanoma cell

lines, C8161, WM983C and 1205Lu [15,17,18], which have mean cell cycle durations of approximately 18, 27 and 36 h, respectively [15]. Four independent experiments are performed for each cell line. Live-cell images are acquired at 15 min intervals over 48 h.

Images from one position in a single well of a FUCCI-C8161 proliferation assay at 7, 16, 25 and 34 h show red, yellow or green nuclei corresponding to the phases G1, eS or S/G2/M (figure 1*e–h*). We quantify the population growth by counting the total number of cells in each image (electronic supplementary material, S1) to give $M(t)$ at time t (figure 1*i*). The total number of cells appears to grow exponentially over 48 h, supported by the best fit of equation (1.1) (electronic supplementary material, S1) since we have $R^2 = 0.99$ from the linear regression of $\ln M(t)$ versus t. The temporal variations in the numbers of cells in the subpopulations $R(t)$, $Y(t)$ and $G(t)$ with red, yellow or green nuclei (figure 1*j*), respectively, where $M(t) = R(t) + Y(t) + G(t)$, are oscillatory. In an asynchronous population, the subpopulations would exhibit monotone growth. The oscillations we observe, however, reveal that the cells are partially synchronous.

To explore the inherent synchronization further, we group cells in eS and S/G2/M together, since eS is part of S, and consider the ratio $Q(t) = R(t)/(Y(t) + G(t))$ (figure 1*k*). Synchronization is clearly evident in the oscillatory nature of $Q(t)$. Note that the troughs at 7 and 25 h and the peaks at 16 and 34 h are separated by 18 h, which is the approximate cell cycle time for C8161. We can visualize the oscillations in these two subpopulations (figure 1*e–h*), where the ratio of the number of red cells to the number of yellow and green cells is lower at 7 and 25 h and higher at 16 and 34 h. Equation (1.1) and related generalizations [8] cannot account for the oscillations in these subpopulations. Similar observations are made for further examples of this cell line, and the two additional cell lines (electronic supplementary material, S1). We quantitatively confirm the presence of oscillations in $Q(t)$, arising from inherent synchronization, for all 90 datasets by calculating the discrete Fourier transform of the $Q(t)$ signal, and identifying the dominant frequencies (electronic supplementary material, S1). These results confirm that all 90 experimental replicates display oscillatory subpopulations that are inconsistent with traditional exponential and logistic growth models.

2.2. Multi-stage mathematical model

We employ a multi-stage model of cell proliferation [19] which can describe synchronous populations. The model assumes that the cell cycle durations follow a hypoexponential distribution, which consists of a series of independent exponential distributions with different rates. To apply this model, we partition the cell cycle into k stages, P_i for $i = 1, \ldots, k$, where the duration of each P_i is exponentially distributed with mean μ_i. If $\mathcal{T}$ is the mean cell cycle time then $\sum_{i=1}^{k} \mu_i = \mathcal{T}$. The stages P_i do not necessarily correspond to phases of the cell cycle, but instead are a mathematical device which allows control over the variance of cell cycle phase durations in the multi-stage model, whereby more stages correspond to less variance in the phase durations for a cell population. If we let the transition rates be $\lambda_i = 1/\mu_i$ and consider the partitioned cell cycle $P_1 \xrightarrow{\lambda_1} P_2 \xrightarrow{\lambda_2} \cdots \xrightarrow{\lambda_{k-1}} P_k \xrightarrow{\lambda_k} 2P_1$, we arrive at a system of differential equations describing the mean population $M_i(t)$ in each stage [19],

$$\frac{\mathrm{d}M_i(t)}{\mathrm{d}t} = \begin{cases} 2\lambda_k M_k(t) - \lambda_1 M_1(t), & \text{for } i = 1, \\ \lambda_{i-1} M_{i-1}(t) - \lambda_i M_i(t), & \text{for } i = 2, \ldots, k. \end{cases} \tag{2.1}$$

Note that $M(t) = \sum_{i=1}^{k} M_i(t)$. If $k = 1$, equation (2.1) simplifies to equation (1.1). Within the 48 h duration of our experiments, none of the cell lines exhibits contact inhibition of proliferation, consistent with the typical loss of contact inhibition in cancer cells [20]. Consequently, a carrying capacity is not incorporated into the model.

We solve equation (2.1) numerically with the forward Euler method, and estimate the parameters by fitting the solution to our experimental data (electronic supplementary material, S1). Using 18 stages for each of the three cell cycle phases described by FUCCI, giving $k = 54$, we obtain $M(t)$ (figure 1*i*), $R(t)$, $Y(t)$, $G(t)$ (figure 1*j*) and $Q(t)$ (figure 1*k*), which all correspond well with the experimental data. In particular, the multi-stage model replicates the oscillations in $R(t)$, $Y(t)$, $G(t)$ and $Q(t)$, a feature that is not possible with traditional exponential models. While the multi-stage model can replicate the oscillatory subpopulations, the model is unable to predict all features of the inherent synchronization in a cell proliferation experiment due to variable initial conditions, as the inherent synchronization is a stochastic phenomenon which likely arises from cell division and intercellular interactions. The model can, however, be used to predict general features of the inherent synchronization of each cell line.

3. Conclusion

Our new experimental data demonstrate that cell populations may appear to grow exponentially despite subpopulations exhibiting oscillatory growth arising from normally hidden inherent synchronization. We use standard experimental methods thought to produce asynchronous populations; however, all of our proliferation assays exhibit inherent synchronization. We use FUCCI to track cell cycle progression, which is necessary to confirm cell synchronization. As the standard exponential growth model cannot account for subpopulations with oscillating growth, we use a multi-stage mathematical model of cell proliferation to replicate oscillations in population growth. Our results are important because revealing any synchronization will help to better understand cell cycle-dependent mechanisms, such as changes in migration and drug response. Without quantitative techniques like FUCCI to probe the cell cycle, synchronization and its effects on experimental outcomes and reproducibility may remain hidden.

Data accessibility. All experimental data are available in the electronic supplementary material documents. All algorithms required to replicate this work are available on GitHub at https://github.com/ProfMJSimpson/Vittadello2019.

Authors' contributions. All authors designed the research. S.T.V. performed the research. All authors contributed analytic tools and analysed the data. S.T.V. wrote the manuscript, and all authors approved the final version of the manuscript. N.K.H. and M.J.S. contributed equally.

Competing interests. We declare we have no competing interests.

Funding. N.K.H. is a Cameron fellow of the Melanoma and Skin Cancer Research Institute and is supported by the NHMRC (APP1084893). M.J.S. is supported by the ARC (DP170100474).

Acknowledgements. We thank the editor and four anonymous referees for helpful comments.

References

1. Sherratt JA, Murray JD. 1990 Models of epidermal wound healing. *Proc. R. Soc. Lond. B* **241**, 29–36. (doi:10.1098/rspb.1990.0061)
2. Swanson KR, Bridge C, Murray JD, Alvord EC. 2003 Virtual and real brain tumors: using mathematical modeling to quantify glioma growth and invasion. *J. Neurol. Sci.* **216**, 1–10. (doi:10.1016/j.jns.2003.06.001)
3. Maini PK, McElwain DLS, Leavesley DI. 2004 Traveling wave model to interpret a wound-healing cell migration assay for human peritoneal mesothelial cells. *Tissue Eng.* **10**, 475–482. (doi:10.1089/107632704323061834)
4. Scott JG, Basanta D, Anderson ARA, Gerlee P. 2013 A mathematical model of tumour self-seeding reveals secondary metastatic deposits as drivers of primary tumour growth. *J. R. Soc. Interface* **10**, 20130011. (doi:10.1098/rsif.2013.0011)
5. Sarapata EA, de Pillis LG. 2014 A comparison and catalog of intrinsic tumor growth models. *Bull. Math. Biol.* **76**, 2010–2024. (doi:10.1007/s11538-014-9986-y)
6. Böttcher MA, Dingli D, Werner B, Traulsen A. 2018 Replicative cellular age distributions in compartmentalized tissues. *J. R. Soc. Interface* **15**, 20180272. (doi:10.1098/rsif.2018.0272)
7. Treloar KK, Simpson MJ, McElwain DLS, Baker RE. 2014 Are *in vitro* estimates of cell diffusivity and cell proliferation rate sensitive to assay geometry? *J. Theor. Biol.* **356**, 71–84. (doi:10.1016/j.jtbi.2014.04.026)
8. Tsoularis A, Wallace J. 2002 Analysis of logistic growth models. *Math. Biosci.* **179**, 21–55. (doi:10.1016/S0025-5564(02)00096-2)
9. Sakaue-Sawano A *et al.* 2008 Visualizing spatiotemporal dynamics of multicellular cell-cycle progression. *Cell* **132**, 487–498. (doi:10.1016/j.cell.2007.12.033)
10. Beaumont KA, Hill DS, Daignault SM, Lui GYL, Sharp DM, Gabrielli B, Weninger W, Haass NK. 2016 Cell cycle phase-specific drug resistance as an escape mechanism of melanoma cells. *J. Invest. Dermatol.* **136**, 1479–1489. (doi:10.1016/j.jid.2016.02.805)
11. Otani K, Naito Y, Sakaguchi Y, Seo Y, Takahashi Y, Kikuta J, Ogawa K, Ishii M. 2016 Cell-cycle-controlled radiation therapy was effective for treating a murine malignant melanoma cell line *in vitro* and *in vivo*. *Sci. Rep.* **6**, 30689. (doi:10.1038/srep30689)
12. Bae H, Go YH, Kwon T, Sung BJ, Cha HJ. 2019 A theoretical model for the cell cycle and drug induced cell cycle arrest of FUCCI systems with cell-to-cell variation during mitosis. *Pharm. Res.* **36**, 57. (doi:10.1007/s11095-019-2570-2)
13. Taylor IW, Hodson PJ. 1984 Cell cycle regulation by environmental pH. *J. Cell. Physiol.* **121**, 517–525. (doi:10.1002/jcp.1041210310)
14. Davis PK, Ho A, Dowdy SF. 2001 Biological methods for cell-cycle synchronization of mammalian cells. *BioTechniques* **30**, 1322–1331. (doi:10.2144/01306rv01)
15. Haass NK, Beaumont KA, Hill DS, Anfosso A, Mrass P, Munoz MA, Kinjyo I, Weninger W. 2014 Real-time cell cycle imaging during melanoma growth, invasion, and drug response. *Pigment. Cell. Melanoma Res.* **27**, 764–776. (doi:10.1111/pcmr.12274)
16. Haass NK, Gabrielli B. 2017 Cell cycle-tailored targeting of metastatic melanoma: challenges and opportunities. *Exp. Dermatol.* **26**, 649–655. (doi:10.1111/exd.13303)
17. Vittadello ST, McCue SW, Gunasingh G, Haass NK, Simpson MJ. 2018 Mathematical models for cell migration with real-time cell cycle dynamics. *Biophys. J.* **114**, 1241–1253. (doi:10.1016/j.bpj.2017.12.041)
18. Simpson MJ, Jin W, Vittadello ST, Tambyah TA, Ryan JM, Gunasingh G, Haass NK, McCue SW. 2018 Stochastic models of cell invasion with fluorescent cell cycle indicators. *Physica A* **510**, 375–386. (doi:10.1016/j.physa.2018.06.128)
19. Yates CA, Ford MJ, Mort RL. 2017 A multi-stage representation of cell proliferation as a Markov process. *Bull. Math. Biol.* **79**, 2905–2928. (doi:10.1007/s11538-017-0356-4)
20. Hanahan D, Weinberg RA. 2011 Hallmarks of cancer: the next generation. *Cell* **144**, 646–674. (doi:10.1016/j.cell.2011.02.013)